WARWICK
THE UNIVERSITY OF WARWICK

Manuscript version: Author's Accepted Manuscript
The version presented in WRAP is the author's accepted manuscript and may differ from the published version or Version of Record.

Persistent WRAP URL:
http://wrap.warwick.ac.uk/108766

How to cite:
Please refer to published version for the most recent bibliographic citation information. If a published version is known of, the repository item page linked to above, will contain details on accessing it.

Copyright and reuse:
The Warwick Research Archive Portal (WRAP) makes this work by researchers of the University of Warwick available open access under the following conditions.

Copyright © and all moral rights to the version of the paper presented here belong to the individual author(s) and/or other copyright owners. To the extent reasonable and practicable the material made available in WRAP has been checked for eligibility before being made available.

Copies of full items can be used for personal research or study, educational, or not-for-profit purposes without prior permission or charge. Provided that the authors, title and full bibliographic details are credited, a hyperlink and/or URL is given for the original metadata page and the content is not changed in any way.

Publisher's statement:
Please refer to the repository item page, publisher's statement section, for further information.

For more information, please contact the WRAP Team at: wrap@warwick.ac.uk.

warwick.ac.uk/lib-publications

Mon. Not. R. Astron. Soc. **000**, 1–10 (2018) Printed 6 September 2018 (MN LATEX style file v2.2)

Effects of non-Kozai mutual inclinations on two-planet system stability through all phases of stellar evolution

Dimitri Veras[1,2⋆†], Nikolaos Georgakarakos[3], Boris T. Gänsicke[1,2], Ian Dobbs-Dixon[3]
[1] *Centre for Exoplanets and Habitability, University of Warwick, Coventry CV4 7AL, UK*
[2] *Department of Physics, University of Warwick, Coventry CV4 7AL, UK*
[3] *New York University Abu Dhabi, Saadiyat Island, P.O. Box 129188, Abu Dhabi, UAE*

arXiv:1809.01157v1 [astro-ph.EP] 4 Sep 2018

6 September 2018

ABSTRACT

Previous full-lifetime simulations of single-star multi-planet systems across all phases of stellar evolution have predominately assumed coplanar or nearly-coplanar orbits. Here we assess the consequences of this assumption by removing it and exploring the effect of giant branch mass loss on the stability of two-planet systems with small to moderate non-Kozai (< 40 degrees) relative inclinations. We run nearly 10^4 simulations over 14 Gyr for F-star, A-star and B-star planet hosts, incorporating main sequence stellar masses of 1.5, 2.0, 2.5, 3.0 and 5.0 solar masses, and initial planetary semimajor axis ratios that straddle their three-dimensional Hill stability limits. We find that the near-coplanar assumption can approximate well the stability frequencies and critical separations found for higher inclinations, except around strong mean-motion commensurabilities. Late instabilities – after the star has become a white dwarf – occur throughout the explored mutual inclination range. Consequently, non-Kozai mutual inclination should not be used as a predictive orbital proxy for determining which white dwarf multi-planet systems discovered by *Gaia* should represent high-priority follow-up targets for the detection of metal pollution and planetary debris discs.

Key words: planet and satellites: dynamical evolution and stability – stars: AGB and post-AGB – stars: white dwarfs – methods:numerical – celestial mechanics – minor planets, asteroids: general

1 INTRODUCTION

One way that the *Gaia* mission could transform the field of exoplanetary science is by allowing us to measure the mutual inclinations of the orbits of an ensemble of planets residing a few au from their parent stars (Perryman et al. 2014). For decades, this elusive orbital parameter has inhibited our efforts to constrain dynamics (Butler et al. 1999), and has represented a frustrating extra degree of freedom in multi-body modelling efforts.

Fortunately, *Gaia*'s exoplanet detections and inclination measurements will not be limited to main sequence host stars. The mission will likely also break new ground by discovering exoplanets orbiting white dwarfs at a distance of a few au. Our current wealth of knowledge of white dwarf planetary systems instead arises from the immediate circumstellar environment, within about one Solar radius of the centre of the white dwarf[1]. This knowledge comes in three flavours, as described below, from: (i) atmospheric metal pollution, (ii) planetary debris discs, and (iii) active exo-minor planets.

1.1 White dwarf planetary systems

Metal pollution in white dwarf atmospheres refers to the detection of spectral lines which cannot be intrinsic to the star (Schatzman 1958; Althaus et al. 2010; Koester 2013) and cannot arise from the interstellar medium (Aannestad et al. 1993; Friedrich et al. 2004; Jura 2006; Kilic & Redfield 2007; Farihi et al. 2010). These lines instead indicate metal-rich planetary debris which has been deposited (Wyatt et al. 2014; Brown et al. 2017) in the atmosphere. Over a thousand metal-polluted white dwarfs are now known (Dufour et al. 2007; Kleinman et al. 2013; Gentile Fusillo et al. 2015; Kepler et al. 2015, 2016;

⋆ E-mail: d.veras@warwick.ac.uk
† STFC Ernest Rutherford Fellow
[1] The exceptions include WD 0806-661b (Luhman et al. 2011) – a planet orbiting a white dwarf at several thousand au – and PSR B1620-26b (Sigurdsson et al. 2003) – a circumbinary planet orbiting both a white dwarf and pulsar.

© 2018 RAS

Hollands et al. 2017), and between one-quarter and one-half of all observed white dwarfs are metal-polluted (Zuckerman et al. 2003, 2010; Koester et al. 2014). Twenty different atmospheric metals have been detected, and overall they resemble the bulk Earth in composition (Klein et al. 2010; Gänsicke et al. 2012; Jura & Young 2014; Wilson et al. 2015, 2016; Xu et al. 2017; Harrison et al. 2018; Hollands et al. 2018). Nearly all metal pollution has been sought around single white dwarfs, although confident detections can be made in wide binary systems containing a white dwarf (Veras et al. 2018).

Over 40 metal-polluted white dwarfs are also known to harbour circumstellar planetary debris discs (Farihi 2016). These discs are compact (could fit within the Sun) and predominantly, unlike protoplanetary discs, are disorderly. White dwarf debris discs are variable (Xu & Jura 2014), eccentric and wispy (Manser et al. 2016), and have demonstrated evidence of morphological changes on both decadal (from Gänsicke et al. 2006) and yearly (Dennihy et al. 2018) timescales. Their formation most likely arises from the break-up of minor bodies which have veered into the white dwarf Roche radius (Graham et al. 1990; Jura 2003; Debes et al. 2012; Bear & Soker 2013; Veras et al. 2014a, 2015a) in combination with the migration of rocky fragments (Dong et al. 2010; Veras et al. 2015b) produced from radiative destruction and/or deformation on the giant branch phase (Veras et al. 2014b; Katz 2018). The subsequent evolution of the discs is complex and involves an interplay of gas and dust (Rafikov 2011a,b; Metzger et al. 2012; Kenyon & Bromley 2017a,b; Miranda & Rafikov 2018).

The minor planet break-up scenario has been evidenced directly, and can in fact be seen on a daily basis around the white dwarf WD 1145+017 when in season. Vanderburg et al. (2015) discovered photometric transit curves suggesting that one or more exo-asteroids are in the process of shedding dust and/or gas around this star. This seminal discovery has lead to over 20 more dedicated papers about this system. The object orbiting this white dwarf is the only known exo-minor planet, and its dynamical origin remains an open question.

1.2 Linking with full-lifetime simulations

Despite this uncertainty, major planets are thought to perturb the minor planets into the white dwarf Roche radius[2]. Therefore, understanding how planets evolve over time and stellar phase is crucial, as is determining when gravitational instabilities occur. Although the majority of literature on planet-planet scattering focuses on the main sequence, we are instead interested in the later phases of stellar evolution.

Efforts to study these scenarios have increased markedly over the last decade (Veras 2016a). Post-main-sequence investigations feature models of single-star exoplanetary systems with an asteroid belt (Dong et al. 2010; Bonsor et al. 2011; Debes et al. 2012; Frewen & Hansen 2014; Mustill et al. 2018; Smallwood et al. 2018), single-star exoplanetary systems without an asteroid belt (Debes & Sigurdsson 2002; Veras et al. 2013a; Voyatzis et al. 2013; Mustill et al. 2014; Veras & Gänsicke 2015; Veras et al. 2016; Payne et al. 2016, 2017), and multiple-star exoplanetary systems (Kratter & Perets 2012; Veras & Tout 2012; Mustill et al. 2013; Portegies Zwart 2013; Bonsor & Veras 2015; Hamers & Portegies Zwart 2016; Kostov et al. 2016; Petrovich & Muñoz 2017; Stephan et al. 2017; Veras et al. 2017a,b; Stephan et al. 2018).

One common theme amongst nearly all of the listed papers above is that they either make an assumption of coplanarity, near-coplanarity (mutual inclinations smaller than a couple of degrees), or focus on the high inclination case, where the Kozai-Lidov mechanism acts (Kozai 1962; Lidov 1962; Naoz 2016). Therefore, there is a need to understand how good or bad the assumption of near-coplanarity is with regard to stability across multiple phases of stellar evolution, and explore the full mutual inclination range from $0^\circ - 40^\circ$. As mentioned earlier, our knowledge of the mutual inclination of the multiple exoplanets in a given exosystem is lacking, and being prepared for revelations from *Gaia* will be beneficial.

1.3 This paper

Therefore, this straightforward paper simply aims to assess, qualitatively, the reliability of the near-coplanar assumption, and hence whether it can continue to be applied with confidence to future modelling efforts and exploratory simulations. We do not attempt to cover a wide range of phase space nor provide detailed dynamical analyses. Instead, we have performed a large ensemble ($\sim 10^4$) of CPU-intensive full-lifetime simulations for the simplest case of two circular, inclined planets orbiting a single star that loses mass isotropically (itself a good assumption; Veras et al. 2013b). This paper then acts as a basic extension to both Veras & Armitage (2004), which considered the dynamics of two planets on circular inclined orbits along the main sequence, and Veras et al. (2013a), which investigated two circular coplanar planets through all phases of stellar evolution. We review our knowledge of stability boundaries in Section 2; Section 3 details our simulations, Section 4 characterizes our results, and Section 5 summarizes our conclusions.

2 STABILITY BOUNDARIES

As in any three-body system, there exist analytical criteria to determine the critical separations beyond which the mutual orbits will never cross (Georgakarakos 2008). These criteria describe *Hill stable* configurations, and rely on the allowed parameter space regions from energy and angular momentum considerations (e.g. Marchal & Bozis 1982). For systems of one star and two equal-mass planets on circular orbits, this separation Δ can be expressed explicitly as a function of mutual inclination $i_{\rm mut}$ (Veras & Armitage 2004) as

$$\Delta \approx \epsilon + \eta \sqrt{\left(4 + \frac{\cos^2 i_{\rm mut}}{2}\right)(\epsilon + \chi \eta \mu^{2/3})}$$

[2] Second generation formation of minor planets around white dwarfs remains a possibility (Schleicher & Dreizler 2014; Völschow et al. 2014; Hogg et al. 2018; van Lieshout et al. 2018).

$$+\chi\eta\mu^{2/3} - 3\eta^2\mu\sqrt{\frac{4+\frac{\cos^2 i_{\rm mut}}{2}}{\epsilon+\chi\eta\mu^{2/3}}} \quad (1)$$

where

$$\epsilon = 2 + \cos^2 i_{\rm mut} - \cos i_{\rm mut}\sqrt{8+\cos^2 i_{\rm mut}}, \quad (2)$$

$$\eta = 1 - \frac{\cos i_{\rm mut}}{\sqrt{8+\cos^2 i_{\rm mut}}}, \quad (3)$$

$$\chi = 3\cdot 2^{1/3}\cdot 3^{1/3}, \quad (4)$$

and μ is the planet-star mass ratio. For arbitrarily inclined and eccentric orbits, the criteria may be written as a set of equations to be solved both explicitly and implicitly (Donnison 2006, 2009, 2011) and generalized to include secular and evection processes (Grishin et al. 2017) and the angular momentum deficit (Petit et al. 2018). Although useful, Hill stability criteria are not exact (see Section 6.5 of Veras et al. 2013a) and become progressively conservative and less useful as the mutual inclination increases, particularly near mean motion commensurabilities (Veras & Armitage 2004). Hence, one may instead appeal to stability boundaries approximated by numerical simulations (e.g. Georgakarakos 2013; Petrovich 2015).

Because Hill stability refers only to the situation where orbits cannot cross, it does not take into account situations where the inner planet collides with the star or the outer planet escapes the system. Hence, Hill stability does not represent a proxy for global stability, known as Lagrange instability (Barnes & Greenberg 2006, 2007; Raymond et al. 2009; Veras & Mustill 2013; Marzari 2014). Therefore, Hill stable systems may be globally unstable. Similarly, Hill unstable systems may be globally stable. In this latter case, a mean motion resonance could provide forcing which protects the system.

Regardless of the stability prescription one uses, as the parent star leaves the main sequence, it will shed mass and expand the orbits of accompanying planets (Omarov 1962; Hadjidemetriou 1963; Veras et al. 2011). The stability boundary varies at a different pace than the semimajor axis ratio of the planets, potentially triggering instability (Debes & Sigurdsson 2002). What remains unclear is how the stability boundaries change in the non-coplanar case, which is the focus of this paper.

In the near-coplanar case, the instability may occur during the giant branch phase, but has been shown to predominantly be delayed until the star has become a white dwarf (Veras et al. 2013a). The implications for white dwarf disc creation and pollution are crucial, as described in Section 1. When a planetary orbital period exceeds the stellar mass loss timescale, then the planet's orbital eccentricity can change appreciably (Veras et al. 2011; Adams et al. 2013), providing for an additional factor in stability boundary changes (Voyatzis et al. 2013). However, eccentricity variations due to mass loss need not be considered here, as the majority of known white dwarf planetary system hosts arise from A and F stars (Tremblay et al. 2016). These stars have peak mass loss timescales which are several orders of magnitude greater than planetary orbital periods, for the vast majority of known planets.

3 SIMULATION SETUP

3.1 Initial condition choices

Indeed, observationally motivated by these A-type and F-type progenitors, we adopted main sequence stellar masses of $1.5M_\odot$ and $2.0M_\odot$ for the majority of our simulations, which ran for 14 Gyr.

We also included simulations with higher stellar masses $2.5M_\odot$, $3.0M_\odot$ and $5.0M_\odot$ in order to showcase potentially extreme cases of dynamical evolution. These latter two classes of simulations also run more quickly than those for A and F stars because of their shorter main sequence lifetimes; for details on these differences, see Veras et al. (2013a). We note that in Veras et al. (2013a), computational limitations prevented us from simulating host star masses lower than $3.0M_\odot$; in the intervening five years, these capabilities have improved[3]. In Veras & Armitage (2004), main sequence simulations of inclined planets were run for just 2 Myr, a full four orders of magnitude shorter than the simulations considered here!

As opposed to both Veras & Armitage (2004) and Veras et al. (2013a), here we sampled initial conditions for the planets in a Monte Carlo fashion within particular parameter ranges. Doing so allowed us to add to our sample size at will, which was useful given the computational demands of the simulations. All our simulations featured two planets with initial mutual inclinations between 1° and 40°, because Kozai-Lidov oscillations may occur for inclinations higher than $\arccos(\sqrt{3/5}) \approx 39^\circ$. The initial inner planet semimajor axis was set at 10 au, which is a realistic value and a high-enough value to enable us to complete 10^4 simulations. The initial outer planet semimajor axis was chosen randomly from a uniform distribution within a range that would showcase both stability and instability. The planets' true anomalies were chosen randomly from a uniform distribution across their entire possible ranges. In a small fraction of cases where we explored non-circular orbits, a planet's initial longitude of ascending node was fixed at 0° but its argument of pericentre was chosen randomly from a uniform distribution across all possible values.

In order to facilitate comparison with the outputs from Veras & Armitage (2004) and Veras et al. (2013a), we chose two Jovian-mass planets on circular orbits for our fiducial set of simulations. We achieved the highest resolution for these simulations, completing 800 simulations for each of the five sampled stellar masses (Fig. 1). We also explored other two-planet scenarios: (i) given a pair of Earth-mass planets, we ran 800 simulations for each of three different stellar masses (Fig. 2), and (ii) given a planet pair including one inner Jovian-mass planet and one outer Earth-mass planet, we ran 800 simulations for each of three different stellar masses (Fig. 3). Finally, we ran a low-resolution ensemble of 400 simulations for a main-sequence stellar mass of $5.0M_\odot$ and a pair of two Jovian-mass planets, where the inner one was

[3] Simulating a stellar host with a mass as low as 1.0 $M_\odot$ over $\approx 10^{10}$ yr remains a CPU-intensive challenge, particularly when using the newly-released and more accurate (but slower) code revealed in Mustill et al. (2018). One partial way to circumvent this issue is to begin simulations towards the end of the main sequence (Veras 2016b).

TWO 1.0 JUPITER-MASS PLANETS

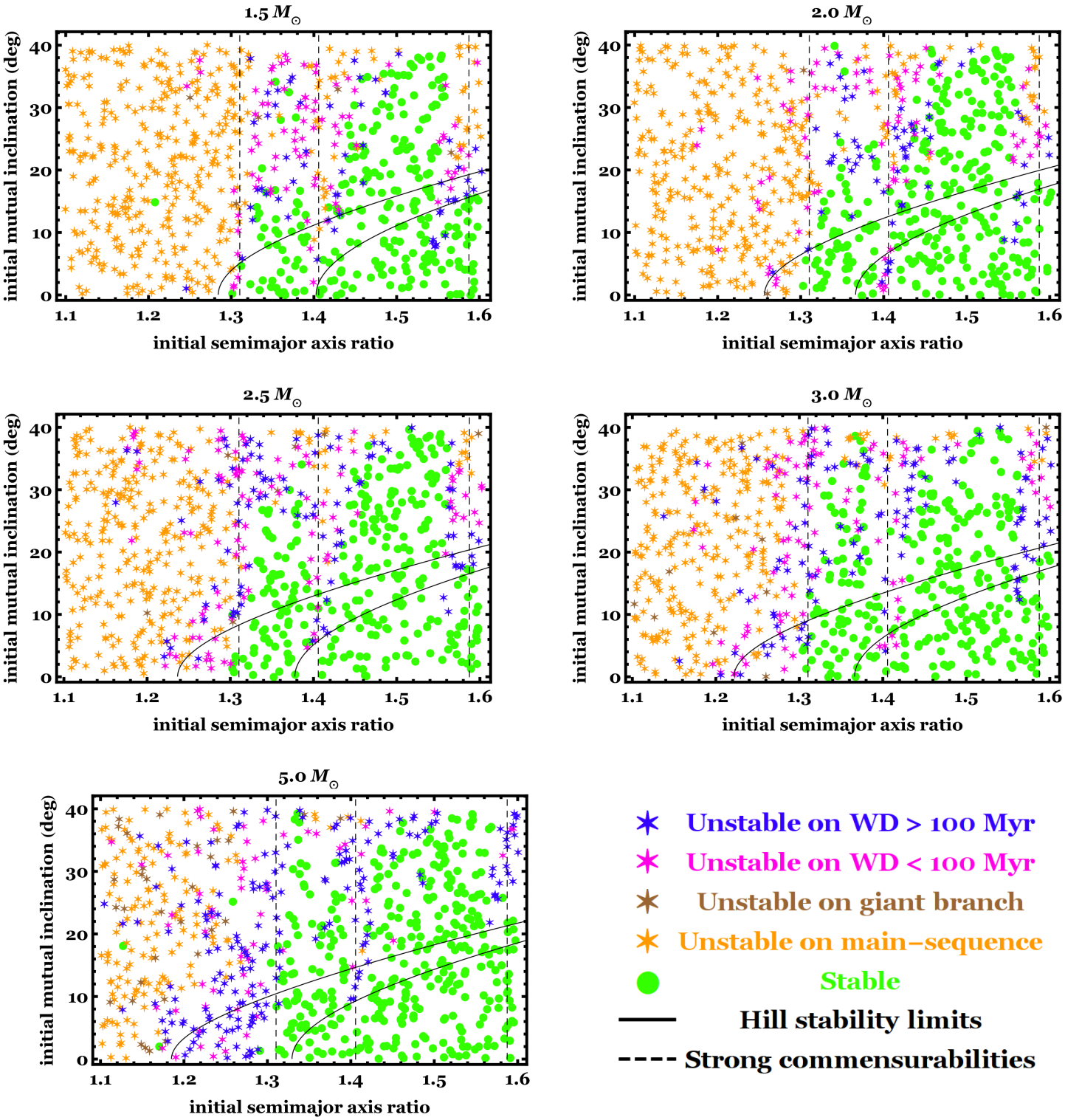

Figure 1. Full-lifetime (14 Gyr) simulations of two $1.0 M_{\rm Jup}$ planets on initially circular orbits around a star with the progenitor main sequence mass stated in the plot title. Dots (which are green) indicate stable simulations, whereas star symbols indicate unstable simulations. Orange and brown stars respectively represent instability on the main sequence and giant branch phases of stellar evolution. Purple and blue stars represent instability on the white dwarf phase when the white dwarf is respectively younger or older than 100 Myr. Overplotted as solid black lines is the Hill stability limit (equation 1) for the main sequence (upper curve) and white dwarf phase (lower curve). Overplotted as vertical dashed lines are, from left to right, the mean motion commensurabilities 3:2, 5:2 and 2:1. The plots illustrate that despite the stability dependencies on initial parameters, (i) late instability along the white dwarf phase occurs throughout the sampled inclination range, and (ii) the assumption of near-coplanarity would be most adequate as a representation for ensemble global stability studies when the planets are away from strong mean-motion commensurabilities or within the Hill stability semimajor axes ratio limits (but external to global chaos from resonance overlap boundary, here near the 3:2 commensurability).

TWO 1.0 EARTH-MASS PLANETS

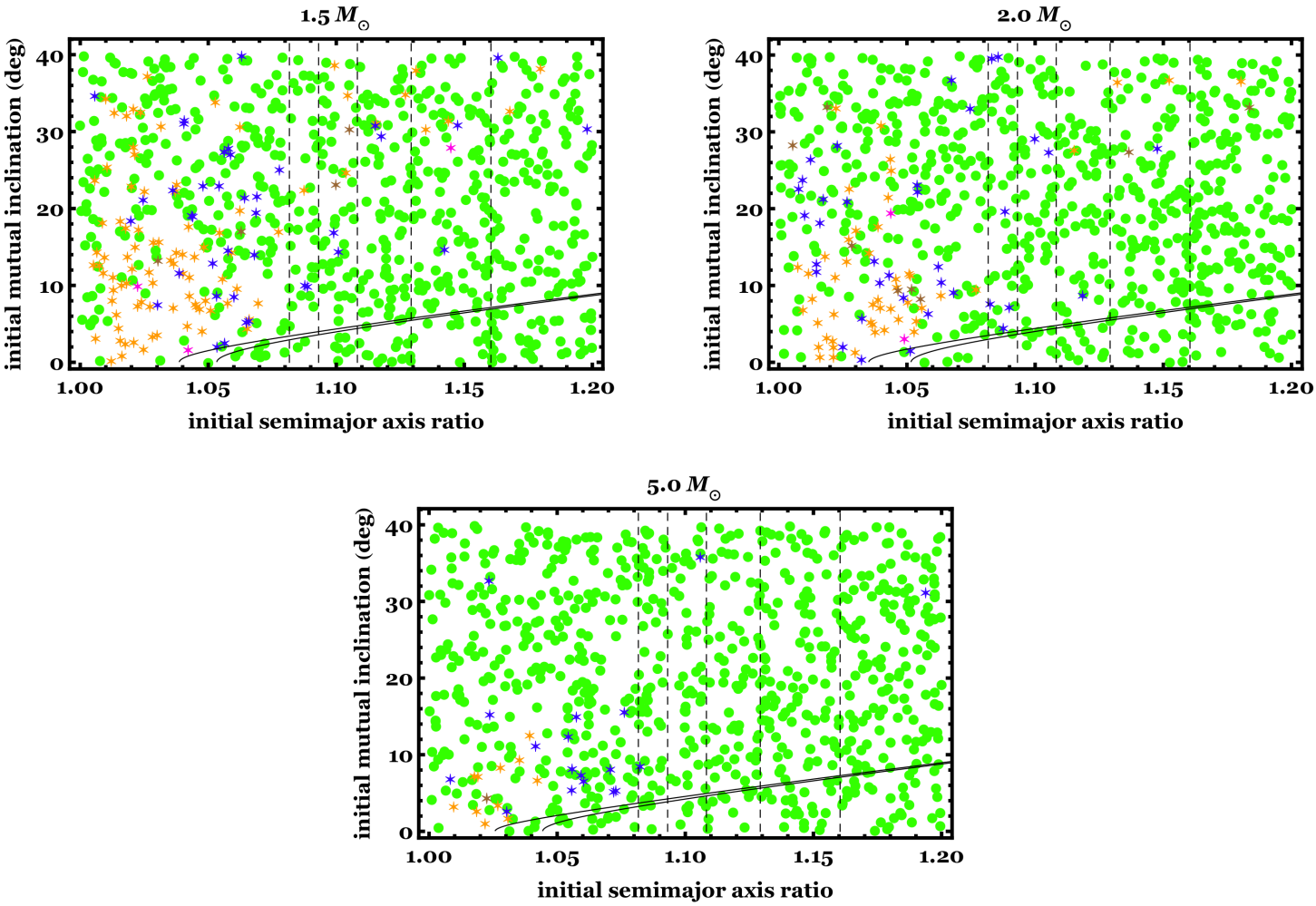

Figure 2. Same as Fig. 1, except for Earth-mass planets and highlighted mean motion commensurabilities of, from left to right, 9:8, 8:7, 7:6, 6:5 and 5:4. In this case, the near-coplanar assumption would excel, except within the Hill stability semimajor axis ratio limit. Late instability on the white dwarf phase can occur for any initial mutual inclination, although that represents a rare outcome for these phase portraits.

on an initially circular orbit, and the outer one's orbit had an initial eccentricity of 0.3 (Fig. 4).

3.2 Simulator

We used the newly-released planetary evolution code used in Mustill et al. (2018) and described in detail in A. Mustill et al. (in prep). This code executes the RADAU integrator to propagate planets forward in time, and is a modified version of the code used in Veras et al. (2013a), where the Bulirsch-Stoer integrator was adopted. That code is itself a modified version of the *Mercury* integration package (Chambers 1999). Stellar evolution is incorporated by interpolating output from the `SSE` code (Hurley et al. 2000) into the timesteps of the planetary propagator.

The `SSE` code was run with its default parameters. These include a stellar metallicity of $Z = 0.02$, a value of 0.5 for the Reimers mass loss coefficient along the giant branch phase, and the inclusion of a superwind along the asymptotic giant branch phase, as prescribed by Vassiliadis & Wood (1993). Although the choice of Reimers mass loss coefficient may qualitatively change evolutionary pathways for Solar-mass stars (Schröder & Cuntz 2005; Veras & Wyatt 2012; Veras 2016b), its importance wanes for higher-mass stars like the ones considered here. In fact, as shown in Fig. 3 of Veras (2016a), of the total mass eventually lost by a main-sequence star of mass $1.5M_\odot$, less than 10 per cent of that loss will occur along the red giant phase; for a star with a main-sequence mass of $2.0M_\odot$, the fraction lost along the giant phase is on the order of just 0.1 per cent.

In the planetary evolution code, the improvement afforded by the RADAU integrator over the Bulirsch-Stoer integrator can be significant (see Appendix A of Mustill et al. 2018), but comes at a price in computational speed. In order to achieve a balance of accuracy and speed, for all our simulations, we adopted a tolerance of 10^{-11}. According to Fig. A1 of Mustill et al. (2018), this tolerance would allow us to accurately track mean anomaly evolution to within about

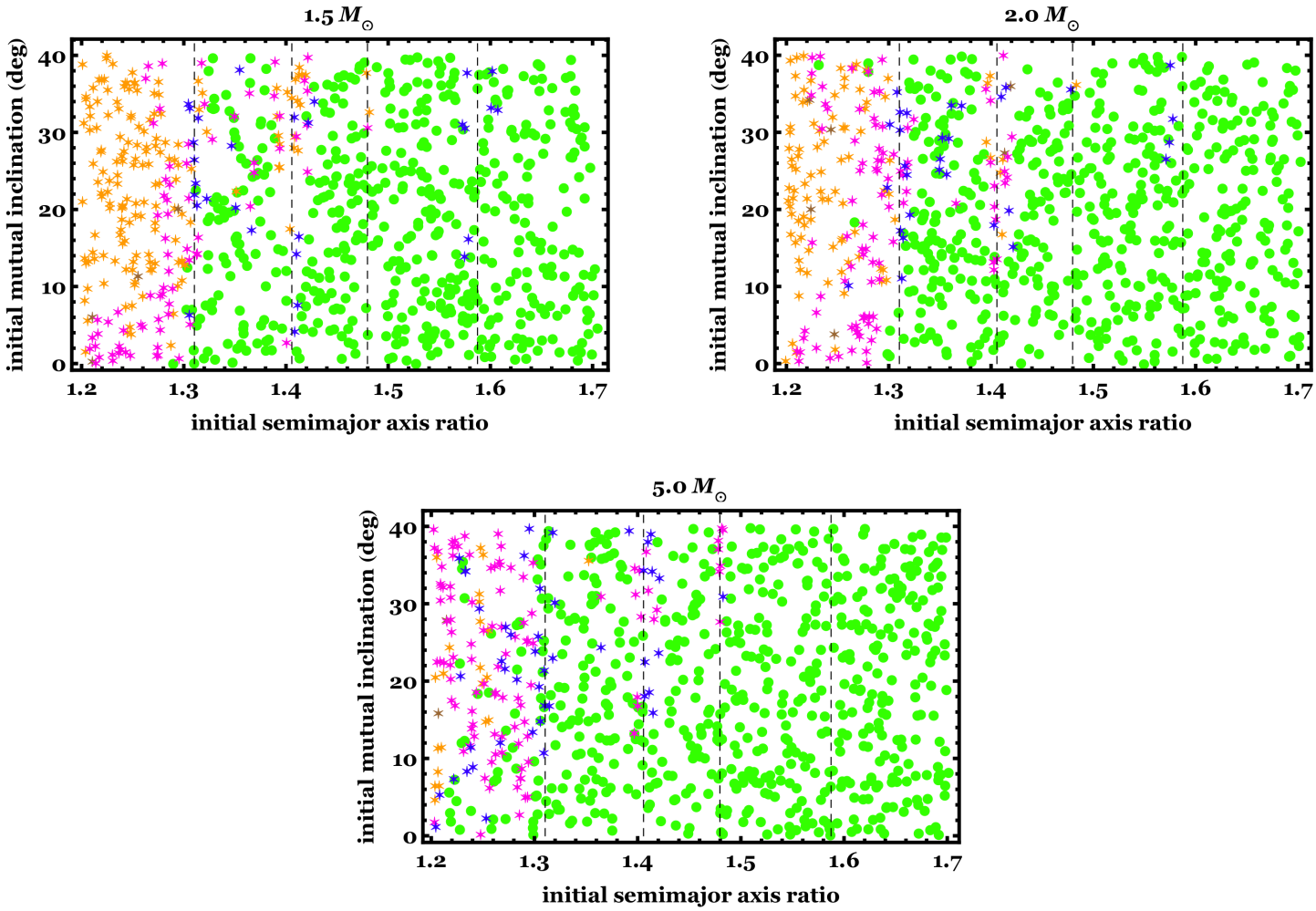

Figure 3. Same as Fig. 2, except for two unequal-mass planets (an inner Jupiter and an outer Earth) and highlighted mean motion commensurabilities of, from left to right, 3:2, 5:3, 9:5 and 2:1. Here, the near-coplanar assumption would remain robust anywhere in semimajor axis ratio phase space except around mean motion commensurabilities. Late instability on the white dwarf phase is more strongly tied to the highlighted commensurabilities than in the other plots, but can still occur for any initial mutual inclination.

a dozen degrees over ≈ 5 Gyr. Such accuracy – which is much higher than what was achieved in Veras et al. (2013a) – aids in the ensemble study of stability performed here, but is perhaps still too low to make detailed conclusions about resonance retention, capture and expulsion across different phases of stellar evolution.

4 RESULTS AND INTERPRETATION

4.1 Summary

We summarise our results with plots of initial mutual inclination versus initial semimajor axis ratio, and use different symbols and colours to indicate stability or instability at different phases (Figs. 1-4). In all plots, we ran 800 simulations, except for Fig. 4, where we ran 400 simulations. We were more interested in vertical trends on the plots rather than horizontal trends, because the latter have already been investigated in detail (Veras et al. 2013a). These plots demonstrate that the vertical trends are weak or nonexistent. Hence, we conclude that instability is largely independent of non-Kozai mutual inclination except close to mean motion commensurabilities.

4.2 Details

Now we provide some details of the plots, which illustrate instability at various times, and distinguish stable systems from unstable systems. By the term "instability" we are referring to a disruption in the system: instantiated either by

planetary escape from the system, or with a collision (between both planets or with the star and planet)[4].

The meaning of the colours and symbols are as follows. Green dots indicate stable systems. Unstable systems, denoted by star symbols, are distinguished by colour: the abundant orange symbols indicate main sequence instability, the rare brown symbols indicate instability on the giant branch phase, and the purple and blue symbols represent instability on the white dwarf phase, for, respectively, white dwarf ages (known as "cooling ages") less and greater than 100 Myr.

This last division was motivated by giant branch mass loss having a well-documented effect of predominantly delaying instability until just after the white dwarf is born; later instability does occurs, but decreases in frequency with time (Veras et al. 2013a; Mustill et al. 2014; Veras & Gänsicke 2015; Veras et al. 2016; Mustill et al. 2018). The later instabilities are particularly important as a way to explain the white dwarf pollution observed in white dwarfs which are Gyrs old (Hollands et al. 2018). The scatter in blue symbols on the plots demonstrate that late instability along the white dwarf phase may occur at any value of the initial mutual inclination, and without a strong preference for low or high values.

This scatter emphasises the sensitivity of the stability of planetary systems to initial conditions. The sensitivity to the initial semimajor axis ratio is seen most starkly at the value where the bulk of the main-sequence instability (orange star symbols) ends. This value lies roughly at the location of the Hill stability boundary for circular orbits ($i_{\rm mut} = 0^\circ$ in equation 1). We have plotted equation (1) in Figs. 1 and 2 as black curves, both for the main sequence mass (upper curve) and white dwarf mass (lower curve). The first figure illustrates that the inclination-dependence of Hill stability for both main sequence and white dwarf systems with Jupiter-mass planets roughly mirrors the trend that instability increases with higher initial mutual inclination.

However, the greater dependence on stability arises from proximity to a strong mean motion resonance. Hence, we have overlayed dashed vertical lines on the plots indicating the locations of commensurabilities of interest due to their strength and location. We chose our commensurabilities in order to (i) demonstrate clear connections between commensurability and instability, and (ii) in cases of near-ubiquitous stability throughout the phase space (Fig. 2), to demonstrate that even the strongest commensurabilities may not affect system stability. As the accuracy and output frequency of our long-term simulations are not quite at a level where a proper resonant analysis could be performed, we are content here to just show proximity to commensurability. Overall, the commensurability locations correspond to strips of instability (star symbols) amidst a sea of stability (green dots).

This trend is clear for the Jupiters in Fig. 1, where from left to right the 3:2, 5:2 and 2:1 commensurabilities are plotted. These commensurabilities were computed strictly from orbital period ratios only, without incorporating the time evolution of the longitudes of ascending node, nor the planet masses. Note that regardless of the fact that inclination-based resonances must be of at least order two, both the 3:2 and 2:1 commensurabilities clearly correlate with instability. One potential reason is that around these locations, the resonant angles associated with the 6:4, 9:6, 4:2 or 6:3 commensurabilities could be librating (Veras 2007). Further, the 3:2 commensurability lies close to the circular Hill stable limit, and both are related through resonant overlap (Wisdom 1980; Mardling 2008; Quillen 2011; Deck et al. 2013; Ramos et al. 2015; Hadden & Lithwick 2018).

In fact, for the Earths in Fig. 2, the lack of correlation between the green dots (stable systems) and the first-order mean motion commensurabilities (plotted from left to right are the 9:8, 8:7, 7:6, 6:5 and 5:4 commensurabilities) illustrates either that (i) resonant overlap has washed away any observable trend between nominal commensurability locations and instabilities, or (ii) simply that the associated first-order resonant librating angles cannot be inclination-based. In contrast, the trend is strongest in Fig. 3 (from left to right, the 3:2, 5:3, 9:5 and 2:1 commensurabilities are drawn), which features one Jupiter and one Earth. Unequal mass objects allow for stronger signatures of resonant capture because in this case resonant angles are more likely to librate, as they could include some terms which may be neglected. The most striking trend is the narrowly-confined band of instability for the $5.0 M_\odot$ main sequence progenitor. As a fourth-order resonance, and the weakest highlighted on the figure, the libration width in initial semimajor axis ratio space would be the smallest.

Despite these trends, the plots demonstrate that non-Kozai mutual inclination represents a weak distinguishing factor in the stability of full-lifetime planetary systems. Adding an additional degree of freedom such as eccentricity complicates the dependency further. As an example, consider Fig. 4, where we set the initial eccentricity of the outer planet to 0.3. As a result, the stability limits and commensurability locations change, yielding a fuzzier semimajor axis ratio boundary between stability and instability. Nevertheless, no vertical trends are apparent, reinforcing the conclusions of this study.

Ensemble studies like this one could always benefit from a finer sampling of phase space and greater integrator accuracy. Georgakarakos (2013) created a detailed phase portrait in mass and mutual inclination space of stability for two planets orbiting a main sequence star. By integrating some systems for up to 10^7 orbits of the outer planet, he showed that mutual inclination does affect the stability boundary across all mutual inclinations from 0° to 180°, but only weakly when $i_{\rm mut} \approx 0^\circ - 40^\circ$. Here, in our more broad study, we place all unstable main sequence systems in the same category, despite the different main sequence lifetimes of the sampled progenitor star masses. Future studies could involve not just a more expansive sampling of the phase space, but also the inclusion of more planets, and an inclination-based extension to the planet packing hypothesis (Chambers et al. 1996; Raymond et al. 2009; Fang & Margot 2013; Kratter & Shannon 2014; Pu & Wu 2015; Hwang et al. 2017), particularly on the post-main-sequence (Veras & Gänsicke 2015; Veras et al. 2016). A different type of extension might involve exploring how mutual

[4] We define the escape boundary as the Hill ellipsoid surrounding the star, as in previous studies (Shannon et al. 2014; Veras et al. 2014c; Veras 2016b). "Hill ellipsoid" here refers to the region within the Galactic Disc which is 8 kpc away from the Galactic centre where objects are gravitationally attracted to the star (Veras & Evans 2013; Veras et al. 2014d).

TWO 1.0 JUPITER-MASS PLANETS, WITH THE OUTER ONE ECCENTRIC

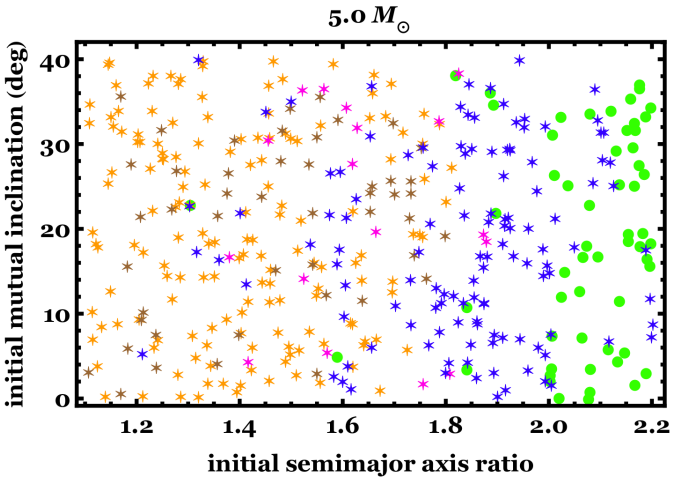

Figure 4. Same as Fig. 1, except the outer planet's orbit is given an initial eccentricity of 0.3. Although the horizontal scatter in the stability boundaries is more evident in this plot, it reinforces the main conclusions of the paper.

inclination affects the generation of high eccentricities (required to generate white dwarf metal pollution) from particular mean motion resonances (Pichierri et al. 2017), secular resonances (Smallwood et al. 2018) and periodic orbits (Antoniadou & Veras 2016).

5 SUMMARY

The *Gaia* mission will, likely for the first time, (i) discover planets orbiting white dwarfs at distances of a few au, and (ii) allow the mutual inclination of multiple planets to be measured for an ensemble of systems. However, no dedicated exploration of the effects of non-Kozai mutual inclinations in multi-planet systems across all phases of stellar evolution is available. This paper has attempted to fill this gap, at least with an initial statistical study, partly to help assess the goodness of the near-coplanar assumption which has predominately been applied until now. We performed about 10^4 computationally-intensive simulations of two-planet systems which ran for 14 Gyr across all phases of stellar evolution, and utilised an accurate RADAU code with an adopted tolerance of 10^{-11} (Mustill et al. 2018; A. Mustill in prep). We found that instabilities occurring around old white dwarfs can be triggered from any initial mutual inclination between 0° and 40°, and that instability along any post-main-sequence phase is a weak function of initial mutual inclination, but a strong function of proximity to mean motion commensurability. Consequently, a measured mutual inclination alone would not a reliable indicator of the evolutionary history and fate of a specific white dwarf multi-planet system.

ACKNOWLEDGEMENTS

We thank the referee for their useful comments, which have improved the manuscript. DV gratefully acknowledges the support of the STFC via an Ernest Rutherford Fellowship (grant ST/P003850/1), and has received, along with BTG, funding from the European Research Council under the European Union's Seventh Framework Programme (FP/2007-2013)/ERC Grant Agreement n. 320964 (WDTracer).

REFERENCES

Aannestad, P. A., Kenyon, S. J., Hammond, G. L., & Sion, E. M. 1993, AJ, 105, 1033
Adams, F. C., Anderson, K. R., & Bloch, A. M. 2013, MNRAS, 432, 438
Althaus, L. G., Córsico, A. H., Isern, J., & García-Berro, E. 2010, ARA&A, 18, 471
Antoniadou, K. I., & Veras, D. 2016, MNRAS, 463, 4108
Barnes, R., & Greenberg, R. 2006, ApJL, 647, L163
Barnes, R., & Greenberg, R. 2007, ApJL, 665, L67
Bear, E., & Soker, N. 2013, New Astronomy, 19, 56
Bonsor, A., Mustill, A. J., & Wyatt, M. C. 2011, MNRAS, 414, 930
Bonsor, A., & Veras, D. 2015, MNRAS, 454, 53
Brown, J. C., Veras, D., & Gänsicke, B. T. 2017, MNRAS, 468, 1575
Butler, R. P., Marcy, G. W., Fischer, D. A., Brown, T. M., Contos, A. R., Korzennik, S. G., Nisenson, P., Noyes, R. W. 1999, ApJ, 526, 916
Chambers, J. E., Wetherill, G. W., & Boss, A. P. 1996, Icarus, 119, 261
Chambers, J. E. 1999, MNRAS, 304, 793
Debes, J. H., & Sigurdsson, S. 2002, ApJ, 572, 556
Debes, J. H., Walsh, K. J., & Stark, C. 2012, ApJ, 747, 148
Deck, K. M., Payne, M., & Holman, M. J. 2013, ApJ, 774, 129
Dennihy, E., Clemens, J. C., Dunlap, B. H., Fanale, S. M., Fuchs, J. T., Hermes, J. J. 2018, ApJ, 854, 40
Dong, R., Wang, Y., Lin, D. N. C., & Liu, X.-W. 2010, ApJ, 715, 1036
Donnison, J. R. 2006, MNRAS, 369, 1267
Donnison, J. R. 2009, Planetary and Space Science, 57, 771
Donnison, J. R. 2011, MNRAS, 415, 470
Dufour, P., Bergeron, P., Liebert, J., et al. 2007, ApJ, 663, 1291
Fang, J., & Margot, J.-L. 2013, ApJ, 767, 115
Farihi, J., Barstow, M. A., Redfield, S., Dufour, P., & Hambly, N. C. 2010, MNRAS, 404, 2123
Farihi, J. 2016, New Astronomy Reviews, 71, 9
Frewen, S. F. N., & Hansen, B. M. S. 2014, MNRAS, 439, 2442
Friedrich, S., Jordan, S., & Koester, D. 2004, A&A, 424, 665
Gänsicke, B. T., Marsh, T. R., Southworth, J., & Rebassa-Mansergas, A. 2006, Science, 314, 1908
Gänsicke, B. T., Koester, D., Farihi, J., et al. 2012, MNRAS, 424, 333
Gentile Fusillo, N. P., Gänsicke, B. T., & Greiss, S. 2015, MNRAS, 448, 2260
Georgakarakos, N. 2008, Celestial Mechanics and Dynamical Astronomy, 100, 151

Georgakarakos, N. 2013, New Astronomy, 23, 41
Graham, J. R., Matthews, K., Neugebauer, G., & Soifer, B. T. 1990, ApJ, 357, 216
Grishin, E., Perets, H. B., Zenati, Y., & Michaely, E. 2017, MNRAS, 466, 276
Hadden, S., & Lithwick, Y. 2018, arXiv:1803.08510
Hadjidemetriou, J. D. 1963, Icarus, 2, 440
Hamers, A. S., & Portegies Zwart, S. F. 2016, MNRAS, 462, L84
Harrison, J. H. D., Bonsor, A., & Madhusudhan, N. 2018, MNRAS, 479, 3814.
Hogg, M. A., Wynn, G. A., & Nixon, C. 2018, MNRAS, 479, 4486
Hollands, M. A., Koester, D., Alekseev, V., Herbert, E. L., & Gänsicke, B. T. 2017, MNRAS, 467, 4970
Hollands, M. A., Gänsicke, B. T., & Koester, D. 2018, MNRAS, 477, 93.
Hurley, J. R., Pols, O. R., & Tout, C. A. 2000, MNRAS, 315, 543
Hwang, J. A., Steffen, J. H., Lombardi, J. C., Jr., & Rasio, F. A. 2017, MNRAS, 470, 4145
Jura, M. 2003, ApJL, 584, L91
Jura, M. 2006, ApJ, 653, 613
Jura, M., & Young, E. D. 2014, Annual Review of Earth and Planetary Sciences, 42, 45
Katz, J. I. 2018, MNRAS, 478, L95
Kenyon, S. J., & Bromley, B. C. 2017a, ApJ, 844, 116
Kenyon, S. J., & Bromley, B. C. 2017b, ApJ, 850, 50
Kepler, S. O., Pelisoli, I., Koester, D., et al. 2015, MNRAS, 446, 4078
Kepler, S. O., Pelisoli, I., Koester, D., et al. 2016, MNRAS, 455, 3413
Kilic, M., & Redfield, S. 2007, ApJ, 660, 641
Klein, B., Jura, M., Koester, D., Zuckerman, B., & Melis, C. 2010, ApJ, 709, 950
Kleinman, S. J., Kepler, S. O., Koester, D., et al. 2013, ApJS, 204, 5
Koester, D. 2013, Planets, Stars and Stellar Systems. Volume 4: Stellar Structure and Evolution, 4, 559
Koester, D., Gänsicke, B. T., & Farihi, J. 2014, A&A, 566, A34
Kostov, V. B., Moore, K., Tamayo, D., Jayawardhana, R., & Rinehart, S. A. 2016, ApJ, 832, 183
Kozai, Y. 1962, AJ, 67, 591
Kratter, K. M., & Perets, H. B. 2012, ApJ, 753, 91
Kratter, K. M., & Shannon, A. 2014, MNRAS, 437, 3727
Lidov, M. L. 1962, Planetary and Space Science, 9, 719
Luhman, K. L., Burgasser, A. J., & Bochanski, J. J. 2011, ApJL, 730, L9
Manser, C. J., Gänsicke, B. T., Marsh, T. R., et al. 2016, MNRAS, 455, 4467
Marchal, C., & Bozis, G. 1982, Celestial Mechanics, 26, 311
Mardling, R. A. 2008, Dynamical Evolution of Dense Stellar Systems, 246, 199
Marzari, F. 2014, MNRAS, 442, 1110
Metzger, B. D., Rafikov, R. R., & Bochkarev, K. V. 2012, MNRAS, 423, 505
Miranda, R., & Rafikov, R. R. 2018, ApJ, 857, 135.
Mustill, A. J., Marshall, J. P., Villaver, E., et al. 2013, MNRAS, 436, 2515
Mustill, A. J., Veras, D., & Villaver, E. 2014, MNRAS, 437, 1404
Mustill, A. J., Villaver, E., Veras, D., Gänsicke, B. T., Bonsor, A. 2018, MNRAS, 476, 3939.
Naoz, S. 2016, ARA&A, 54, 441
Omarov, T. B. 1962, Izv. Astrofiz. Inst. Acad. Nauk. KazSSR, 14, 66
Payne, M. J., Veras, D., Holman, M. J., Gänsicke, B. T. 2016, MNRAS, 457, 217
Payne, M. J., Veras, D., Gänsicke, B. T., & Holman, M. J. 2017, MNRAS, 464, 2557
Perryman, M., Hartman, J., Bakos, G. Á., Lindegren, L. 2014, ApJ, 797, 14.
Petit, A. C., Laskar, J., & Boué, G. 2018, arXiv:1806.08869
Petrovich, C. 2015, ApJ, 808, 120
Petrovich, C., & Muñoz, D. J. 2017, ApJ, 834, 116
Pichierri, G., Morbidelli, A., & Lai, D. 2017, A&A, 605, A23
Portegies Zwart, S. 2013, MNRAS, 429, L45
Pu, B., & Wu, Y. 2015, ApJ, 807, 44
Quillen, A. C. 2011, MNRAS, 418, 1043
Rafikov, R. R. 2011a, MNRAS, 416, L55
Rafikov, R. R. 2011b, ApJL, 732, L3
Ramos, X. S., Correa-Otto, J. A., & Beaugé, C. 2015, Celestial Mechanics and Dynamical Astronomy, 123, 453
Raymond, S. N., Barnes, R., Veras, D., et al. 2009, ApJL, 696, L98
Schatzman, E. L. 1958, Amsterdam, North-Holland Pub. Co.; New York, Interscience Publishers, 1958
Schleicher, D. R. G., & Dreizler, S. 2014, A&A, 563, A61
Schröder, K.-P., & Cuntz, M. 2005, ApJ, 630, L73.
Shannon, A., Clarke, C., & Wyatt, M. 2014, MNRAS, 442, 142.
Sigurdsson, S., Richer, H. B., Hansen, B. M., Stairs, I. H., & Thorsett, S. E. 2003, Science, 301, 193
Smallwood, J. L., Martin, R. G., Livio, M., & Lubow, S. H. 2018, MNRAS, 480, 57
Stephan, A. P., Naoz, S., & Zuckerman, B. 2017, ApJL, 844, L16
Stephan, A. P., Naoz, S., & Gaudi, B. S. 2018, Submitted to AAS Journals, arXiv:1806.04145
Tremblay, P.-E., Cummings, J., Kalirai, J. S., Gänsicke, B. T., Gentile-Fusillo, N., Raddi, R. 2016, MNRAS, 461, 2100
van Lieshout, R., Kral, Q., Charnoz, S., et al. 2018, MNRAS, 480, 2784.
Vanderburg, A., Johnson, J. A., Rappaport, S., et al. 2015, Nature, 526, 546
Vassiliadis, E., & Wood, P. R. 1993, ApJ, 413, 641
Veras, D., & Armitage, P. J. 2004, Icarus, 172, 349
Veras, D. 2007, Celestial Mechanics and Dynamical Astronomy, 99, 197
Veras, D., Wyatt, M. C., Mustill, A. J., Bonsor, A., & Eldridge, J. J. 2011, MNRAS, 417, 2104
Veras, D., & Tout, C. A. 2012, MNRAS, 422, 1648
Veras, D., & Wyatt, M. C. 2012, MNRAS, 421, 2969
Veras, D., & Evans, N. W. 2013, MNRAS, 430, 403.
Veras, D., Mustill, A. J., Bonsor, A., & Wyatt, M. C. 2013a, MNRAS, 431, 1686
Veras, D., Hadjidemetriou, J. D., & Tout, C. A. 2013b, MNRAS, 435, 2416
Veras, D., & Mustill, A. J. 2013, MNRAS, 434, L11
Veras, D., Leinhardt, Z. M., Bonsor, A., Gänsicke, B. T. 2014a, MNRAS, 445, 2244

Veras, D., Jacobson, S. A., Gänsicke, B. T. 2014b, MNRAS, 445, 2794
Veras, D., Shannon, A., & Gänsicke, B. T. 2014c, MNRAS, 445, 4175.
Veras, D., Evans, N. W., Wyatt, M. C., et al. 2014d, MNRAS, 437, 1127.
Veras, D., Gänsicke, B. T. 2015, MNRAS, 447, 1049
Veras, D., Leinhardt, Z. M., Eggl, S., Gänsicke, B. T. 2015a, MNRAS, 451, 3453
Veras, D., Eggl, S., Gänsicke, B. T. 2015b, MNRAS, 451, 2814
Veras, D. 2016a, Royal Society Open Science, 3, 150571
Veras, D. 2016b, MNRAS, 463, 2958
Veras, D., Mustill, A. J., Gänsicke, B. T., et al. 2016, MNRAS, 458, 3942
Veras, D., Georgakarakos, N., Dobbs-Dixon, I., & Gänsicke, B. T. 2017a, MNRAS, 465, 2053
Veras, D., Mustill, A. J., & Gänsicke, B. T. 2017b, MNRAS, 465, 1499
Veras, D., Xu, S., & Rebassa-Mansergas, A. 2018, MNRAS, 473, 2871
Völschow, M., Banerjee, R., & Hessman, F. V. 2014, A&A, 562, A19
Voyatzis, G., Hadjidemetriou, J. D., Veras, D., & Varvoglis, H. 2013, MNRAS, 430, 3383
Wilson, D. J., Gänsicke, B. T., Koester, D., Toloza, O., Pala, A. F., Breedt, E., Parsons, S. G. 2015, MNRAS, 451, 3237
Wilson, D. J., Gänsicke, B. T., Farihi, J., & Koester, D. 2016, MNRAS, 459, 3282
Wisdom, J. 1980, AJ, 85, 1122
Wyatt, M. C., Farihi, J., Pringle, J. E., & Bonsor, A. 2014, MNRAS, 439, 3371
Xu, S., & Jura, M. 2014, ApJL, 792, L39
Xu, S., Zuckerman, B., Dufour, P., Young, E. D., Klein, B., Jura, M. 2017, ApJL, 836, L7
Zuckerman, B., Koester, D., Reid, I. N., Hünsch, M. 2003, ApJ, 596, 477
Zuckerman, B., Melis, C., Klein, B., Koester, D., & Jura, M. 2010, ApJ, 722, 725